3D IMAGE PROCESSING FOR THE STUDY OF THE EVOLUTION OF THE SHAPE OF THE HUMAN SKULL
PRESENTATION OF THE TOOLS AND PRELIMINARY RESULTS

Gérard SUBSOL[1], Bertrand MAFART[2], Marie-Antoinette DE LUMLEY[2], Alain SILVESTRE[3]

Abstract:

We present an automatic method that allows one to visualize and analyze, in three dimensions, the evolution of the shape of the human skull from CT-Scan images. A first algorithm automatically extract the "crest lines" from CT-Scan images of the skull of a modern Man and of a cast of a skull of a prehistoric Man. Those lines correspond to the salient lines of the skull surface. They will be used as landmarks to automatically find the homology points between the two skulls. Based on these couple of matched points, we compute a volumetric transformation that superposes the two skulls. It makes possible to visualize and analyze the evolution of the skull between the prehistoric and the modern Man. We have applied this method to the skull of the Man of Tautavel, dated of about 450,000 years, and we present future applications in facial reconstruction and tridimensional morphometry.

Résumé :

Nous présentons une méthode automatique qui permet de visualiser et d'analyser, en trois dimensions, l'évolution de la forme du crâne humain à partir d'images scanographiques. Un premier algorithme extrait automatiquement des « lignes de crête » à partir des scanographies d'un crâne d'un Homme moderne et du moulage du crâne d'un Homme préhistorique. Ces lignes correspondent aux lignes saillantes de la surface crânienne. Elles servent de repères à un algorithme de mise en correspondance pour trouver automatiquement les points homologues entre les deux crânes. À partir de ces points appariés, on calcule une transformation de l'espace qui superpose les deux crânes. Il est alors possible de visualiser et d'analyser l'évolution du crâne entre l'Homme préhistorique et moderne. Nous appliquons cette méthode au crâne de l'Homme de Tautavel, daté d'environ 450 000 ans, et nous présentons des applications futures en reconstruction faciale et en analyse morphométrique tridimensionnelle.

INTRODUCTION

Computer Tomography Scan images are more and more used in paleo-anthropology (Spoor et al., 2000), especially for the study of the craniofacial massif. The fossil, or its mold, is placed into a Computer Tomography device (see Figure 1) and we obtain, in few minutes, a series of several tens of digital images that represent the successive slices of the anatomical structure. These images are, in general, of a resolution of 512 by 512 pixels which are coded in several thousands of gray levels. They are then "stacked" in order to build up a **three-dimensional image**. CT-Scan devices that are routinely used in medical radiology have a resolution of one millimeter whereas special industrial micro-scanners can reach up to a resolution of one hundred microns (Thompson and Ilerhaus, 1998).

Some image processing algorithms developed for medical imaging (Ayache, 1998) or Computer Assisted Design are applied to extract the surface of the structure from the 3D image and to display it, from any point of view, on the screen of a computer. More generally, these algorithms allows one to interact with the **virtual representations** of the fossils to study them carefully (Weber, 2001), (Zollikofer et al., 1998). The paleontologist can combine the virtual bone fragments to test different reconstruction hypotheses (Kalvin et al., 95), (Thompson & Illerhaus, 1998), (Braun et al., 1999), (Ponce de León & Zollikofer, 1999). New virtual fragments can be created by symmetrizing or adjusting the size of the real fragments. It is also possible to model some taphonomic deformations (Ponce de León & Zollikofer, 1999). The paleontologist is also able to easily visualize the internal structures of the virtual fossils, as the endocranium (Conroy et al., 1990), (Conroy et al., 1998), (Ponce de León & Zollikofer, 1999), the bony labyrinth of the inner ear (Spoor & Zonneveld, 1995), (Thompson & Illerhaus, 1998), (Ponce de León & Zollikofer, 1999), the frontal (Thompson & Illerhaus, 1998), maxillary (Rae & Koppe, 2000) or paranasal (Ponce de León & Zollikofer, 1999) sinuses. Morphometry tools allow to take easily measurements that are very complex to obtain in reality, as the thickness of bones (Zollikofer et al., 1998) or the curvature radius of the semi-circular canals (Spoor & Zonneveld, 1995), (Thompson & Illerhaus, 1998). More generally, it becomes possible to perform a complete three-dimensional study of the shape of the structure (Subsol et al., 2000), (Ponce de León & Zollikofer, 2001). Finally, real replications of the virtual reconstructions can be obtained by some **virtual prototyping** processes as laser stereolithography (Seidler et al., 1997), (Zollikofer et al., 1998).

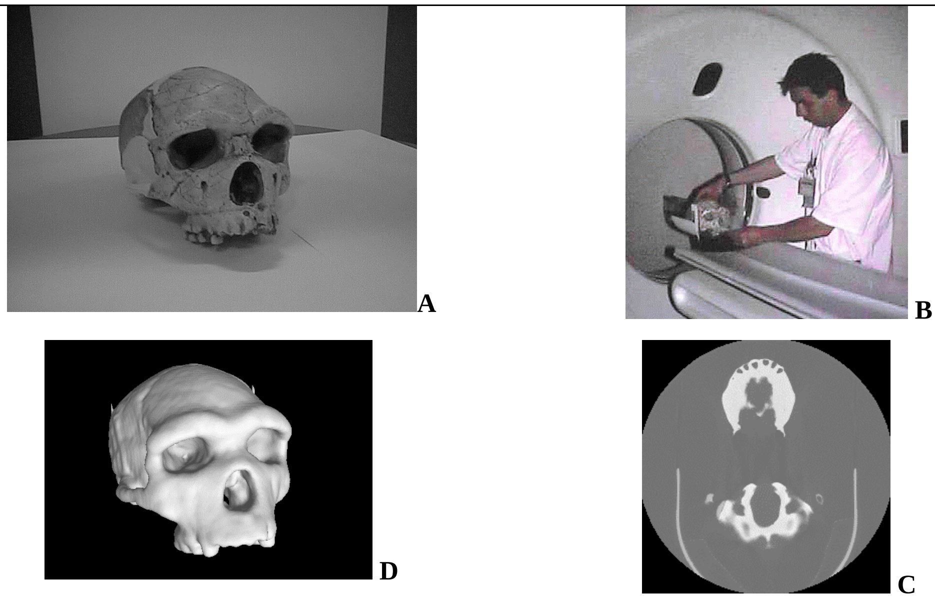

Figure 1*: Obtaining a virtual fossil*
*The anatomical structure or its mold (A) is placed in the CT-Scan device (B). We obtain then a series of several tens of digital images of 512 by 512 pixels in gray levels that correspond to slices (C). It is then possi*ble to *"stack" the slices and to extract the surface of the anatomical structure to visualize it in 3D on a computer screen (D).*

In this paper, we present a new method based on state-of-the-art image processing algorithms that allow to analyze **automatically**, in three dimensions, the evolution of the shape of the human skull. We follow the scheme proposed by d'Arcy Thompson at the beginning of the last century (Thompson, 1917): first, we compute a 3D deformation function between the fossil we want to study and a reference skull; and then, we use tools to visualize this function and to emphasize the differences between the two skulls.

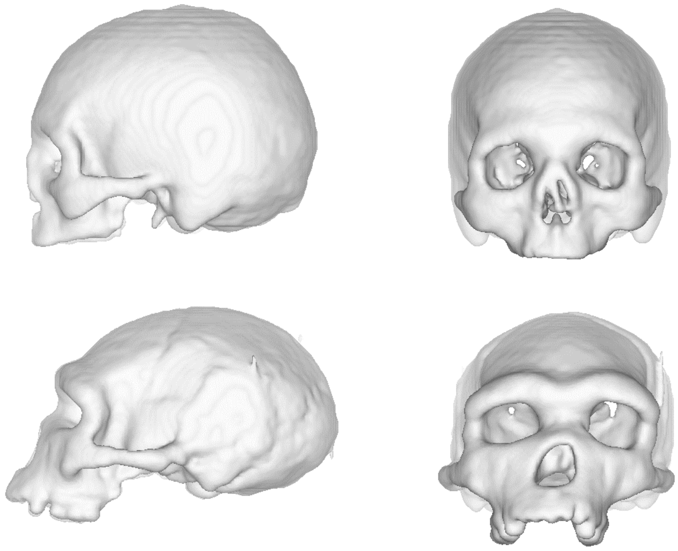

Figure 2*: How to compare the two skulls: Modern Man (up) and Man of Tautavel (bottom)?*
A methodology exists, that consists in computing and analyzing a 3D deformation function between the two skulls.

The main goal of this paper is to assess if the presented automatic image processing tools can be successfully applied. For this purpose, we show some preliminary results that are based on a CT-Scan image of a dry skull of a Modern Man (61 slices with a thickness of 3 mm composed of 512 by 512 pixels of 0.6 by 0.6 mm, data by courtesy of Gérald Quatrehomme, University of Nice, France) and a CT-Scan of a mold of the reconstruction of the skull of the Man of Tautavel (154 slices with a thickness of 1 mm composed of 512 by 512 pixels de 0.5 by 0.5 mm) (see Figure 2). The reconstitution is based on the face (Arago XXI) and the right parietal (Arago XLVII) that were found in the Arago cave at Tautavel in 1971, the left parietal being obtained by symmetry, on a mold of the Swanscombe occipital, and on the temporal bone and its symmetric of Sangiran 17 (Pithecanthropus VIII) (de Lumley, 1982).

PRESENTATION OF THE METHOD

Extraction of feature points and lines

To compute the 3D transformation, we have to find some landmarks on the surface of the skull. They must be defined by an unambiguous mathematical formula to be automatically computed and be anatomically relevant to characterize the structure. We choose **crest lines** (Thirion & Gourdon, 1996), (Subsol et al., 1998) that are defined by the extrema of the principal curvature that has the largest absolute magnitude, along its associated principal direction (see Figure 3). Due to their definition, these lines follow the salient lines of a surface. We can verify this in Figure 4 where the crest lines that were automatically extracted in a CT-Scan of the skull of a Modern Man emphasize the mandible, the orbits, the cheekbones or the temples and also, inside the cranium, the sphenoid and temporal bones as well as the foramen magnum.

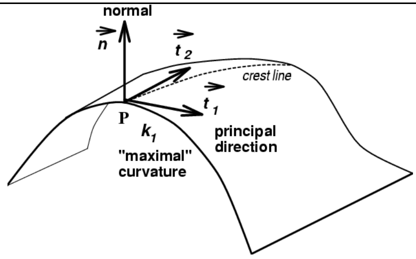

Figure 3*: Mathematical definition of crest lines*

- ***k_1****: maximal principal curvature in absolute value*
- ***t_1****: associated principal direction*

grad k1.t1=0 ⇔ P is a crest point

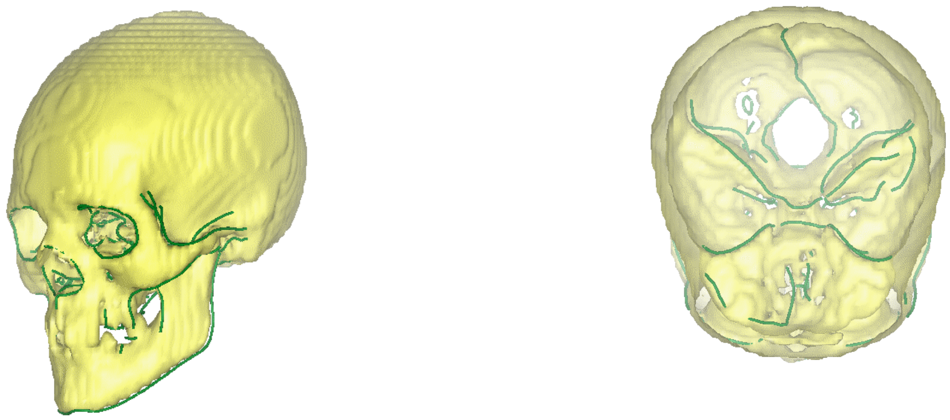

Figure 4*: crest lines automatically extracted in a CT-Scan of the skull of a Modern Man.*
Notice how crest lines emphasize the mandible, the orbits, the cheekbones or the temples and also, inside the cranium, the sphenoid and temporal bones as well as the foramen magnum.

Salient structures are also used by doctors as anatomical landmarks. For example, the crest lines definition is very close to the **ridge lines** described in (Bookstein & Cutting, 1988) (see Figure 5, left) and that are type II landmark in Bookstein's typology (Bookstein, 1991). In Figure 5, right, we display on the same skull the crest lines (in gray) which were automatically extracted and the ridge lines (in black) which were extracted semi-manually under the supervision of an anatomist. The two sets of lines are very close (Thirion et al., 1996), showing that crest lines would have a strong anatomical significance. Notice that ridge lines have also been used in paleontology to compare the Homo Erectus and the Homo Sapiens (Dean, 1993).

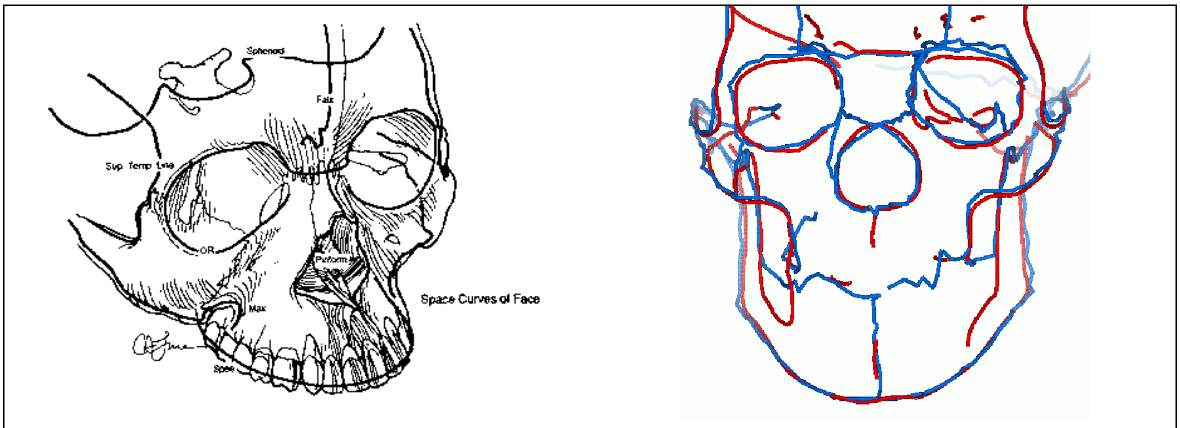

Figure 5*: comparison of ridge lines and crest lines*
Left (excerpt from (Bookstein & Cutting, 1988)): ridge lines are extracted semi-manually under the supervision of an anatomist and are used for applications in craniofacial surgery and paleontology.
Right: the superimposition of crest (in gray) and ridge lines (in black) shows that crest lines have a strong anatomical significance, even if they are based on a mathematical definition.

Registration of feature lines

We extract 536 crest lines composed of 5,756 points on the skull of the Modern Man and 337 crest lines with 5,417 points on the skull of the Man of Tautavel. Now, we have to find the correspondences between these features (see Figure 6). Usually, this is done manually by an anatomist who knows the **biological homology**: two features are put into correspondence if they characterize the same biological functionality. In our case, there is so many points that this is no more possible and we have to design an algorithm to find correspondences automatically. This is a very well known problem in 3D image processing called **registration** (Ayache, 1998). We have developed a method described in (Subsol, 1995), (Subsol et al., 1998) that deforms iteratively and continuously the first set of lines towards the second one in order to superimpose them. At the end of the process, each point P_i, of the first set is matched with the point Q_i of the second set that is the closest, and some inconsistent correspondences are discarded. In our example, the algorithm finds in some minutes, on a standard personal computer, 1,532 points pairings (P_i, Q_i). As they are located all around the inside and outside surfaces of the skull, it becomes really possible to analyze the total structure in three dimensions.

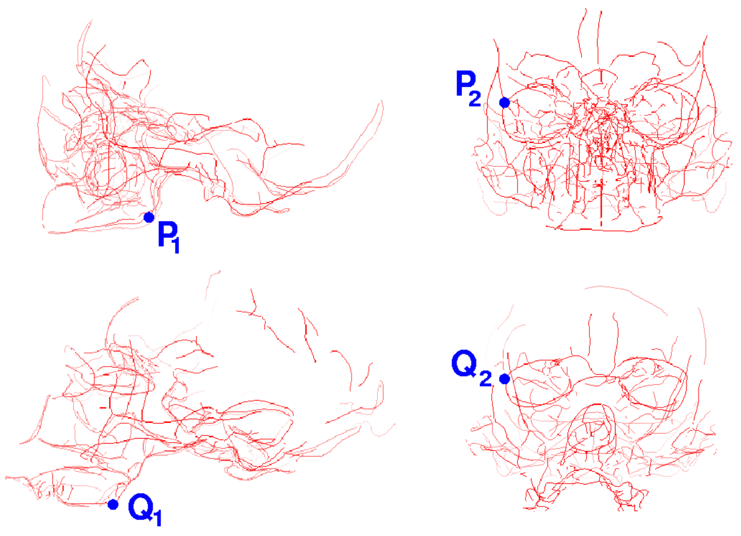

Figure 6*: crest lines automatically extracted and the registration problem. The difficulty is to find the correspondences between these features as, for example, the pairings* (P_1, Q_1) or (P_2, Q_2).
Up: crest lines on the skull of the Modern Man (536 lines and 5756 points)
Bottom: crest lines on the skull of the Man of Tautavel (337 lines and 5417 points).

We checked on several skull data that these registration results are consistent with those obtained by an other automatic method and by a semi-manual method where an anatomist supervises the detection of homologous points (Thirion et al., 1996).

Geometrical normalization

In ontogenetic and evolutive shape transformation studies, we should not take into account differences of position, orientation and size, since they cannot be considered as true morphological differences. This requires to compute the three following transformations between two specimens to compare: the rotation $\underline{\boldsymbol{R}}$, the translation $\underline{\boldsymbol{T}}$ and the scaling $\underline{\boldsymbol{s}}$. Several methods exist to compute $(\underline{\boldsymbol{s}},\underline{\boldsymbol{R}},\underline{\boldsymbol{t}})$ based on pairs of homologous points (P_i,Q_i), as the Procrustes superimposition (Boostein, 1991) or the least-square minimization that leads to:

$$(\underline{\boldsymbol{s}},\underline{\boldsymbol{R}},\underline{\boldsymbol{t}})= \mathrm{Argmin}_{(s,R,t)}\ \Sigma_i \parallel \boldsymbol{sR}\, P_i + \boldsymbol{t} - Q_i \parallel^2)$$

By applying the inverse transformations $(\underline{\boldsymbol{s}}^{-1},\underline{\boldsymbol{R}}^{-1},\underline{\boldsymbol{t}}^{-1})$, we can "normalize" the shape of the second skull that becomes comparable to the first one.

Nevertheless, more complex taphonomic transformations modified the shape of the fossils (Ponce de León & Zollikofer, 1999). Thus, in Figure 7 up, we can notice how the Man of Tautavel's skull is bent. This is due to the fact that it was laid on the side and was compressed by the gravity. We have modeled this deformation by an affine transformation $\underline{\boldsymbol{A}}$. We compute it by the least-square method and applied it to he original skull. We can see in Figure 7, bottom, how the skull was rectified and be made comparable to the skull of the Modern Man.

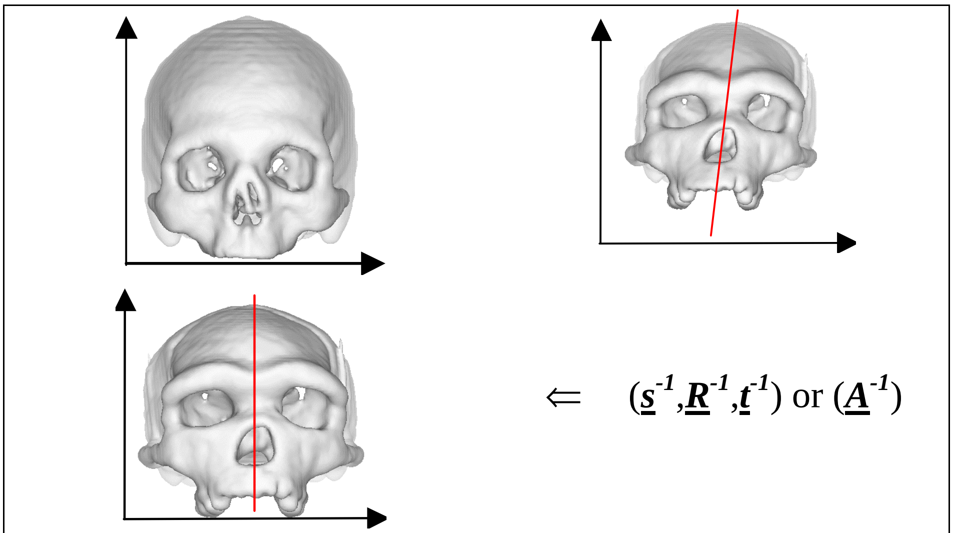

Figure 7: *geometrical normalization of the Man of Tautavel's skull*
This requires to model and compute not only the differences of position, of orientation and size but also some taphonomic deformations. After the normalization (bottom), the skull becomes comparable to the Modern Man's one (up, left).

Another way to recover the bending of the skull consists to extract automatically the mid-sagittal plane (Thirion et al., 2000) and to realign it with the vertical plane. Nevertheless, the knowledge of the in situ orientation of the fossil is indispensable, since similar deformations might be the result of different diagenetic events (Ponce de León & Zollikofer, 1999).

Computing the 3D transformation

Now, we have to compute the 3D transformation between the fossils. The **Thin-Plate Spline** method (Bookstein, 1991), widely used in morphometry, allows to compute such a function that interpolates the displacements of the homologous points (P_i,Q_i) with some mathematical properties of regularity. Nevertheless, interpolation is relevant when the matched points are totally reliable and distributed regularly (for example, with a few points being located manually). In our case, these points are not totally reliable due to possible mismatches of the registration algorithm and are sparse in a few compact areas as they belong to lines. So, we have developed a spline approximation function that is regular enough to minimize the influence of an erroneous matched point (Declerck et al., 1995). The coordinate functions are then computed by a 3D tensor product of B-spline basis functions. To compute this 3D transformation $\underline{\boldsymbol{T}}$, we maximize the weighted sum of an approximation criterion (quadratic distance between $\boldsymbol{T}(P_i)$ and Q_i) and a regularization criterion (minimization of the second order derivatives that corresponds to the "curvature" of the function):

$$\underline{\boldsymbol{T}} = \mathrm{Argmin}_{(T)} \Sigma_i \, \|\boldsymbol{T}(P'_i)Q'_i\|^2 + \rho \iiint (\partial^2\boldsymbol{T}/\partial x^2) + (\partial^2\boldsymbol{T}/\partial x \partial y) + ..$$

The parameter ρ tunes the approximation accuracy or the smoothness of the transformation.

APPLICATION TO THE STUDY OF THE SKULL OF THE MAN OF TAUTAVEL

Analysis of the deformation

We compute the 3D transformation between the Modern Man and the Man of Tautavel based on the features lines. By applying it to a 3D regular mesh, it is possible to visualize the differences between the two structures. We can notice in Figure 8 that the deformed mesh emphasizes the main features of the Man of Tautavel: low skull, receding forehead, protuberant face as well as a an important frontal dissymmetry due to the taphonomic deformations (Mafart et al., 1999).

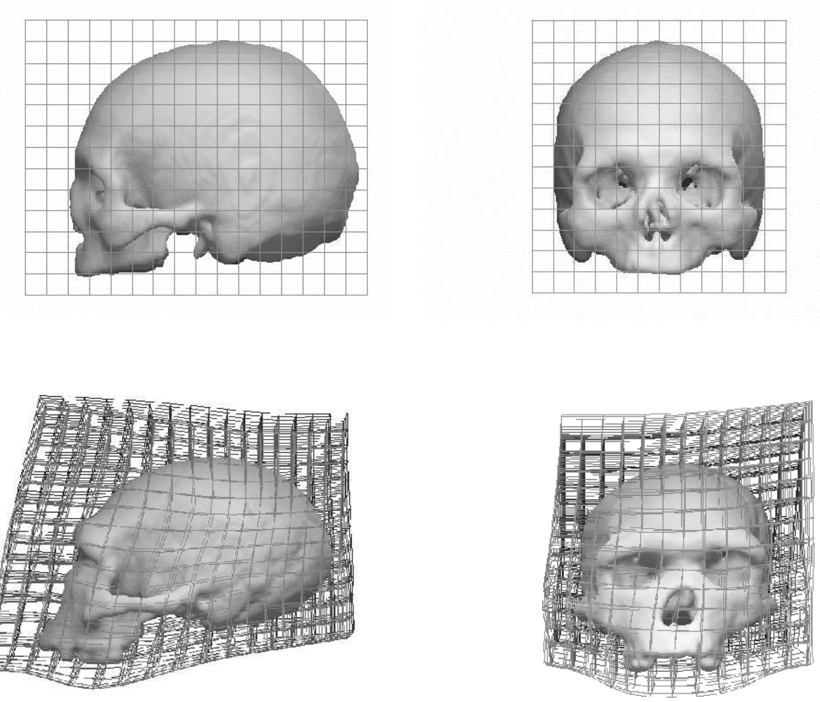

***Figure 8**: 3D transformation between the skull of the Modern Man (up) and of the Man of Tautavel (bottom).*
Notice how the deformed mesh emphasizes the main features of the Man of Tautavel: low skull, receding forehead, protuberant face as well as an important frontal dissymmetry due to the taphonomic deformations.

It is also possible to have a quantitative overview of the deformation. For example, in Figure 9, we colored the surface skull according to the magnitude of the deformation: violet (dark gray) for small displacements and green (light gray) for the largest ones. This shows the importance of the elongation of the face. (Ponce de León & Zollikofer, 2001) proposes other visualization methods as using colors to indicate the direction of the deformation (inward/outward) or displaying the displacement vector field.

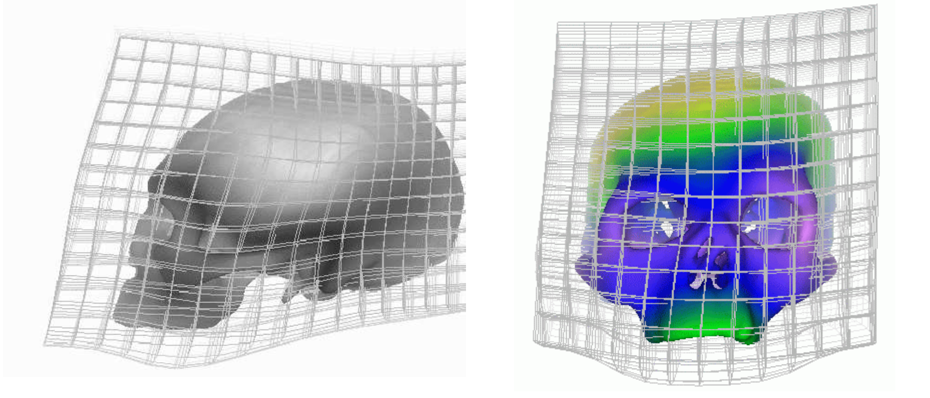

__Figure 9__: a quantitative visualization of the 3D deformation.
The color table on the surface skull characterizes the magnitude of the deformation: violet (dark gray) for small displacements and green (light gray) for the largest ones. This emphasizes, in particular, the importance of the elongation of the face

Facial reconstruction

In (Quatrehomme et al., 1997), we propose an automatic method to perform a 3D facial reconstruction based on the 3D images of an unknown skull and of a reference skull and face (see Figure 10). We register automatically the 3D images by using crest lines and we compute a 3D transformation between the two skulls. If we assume that the shape of the face follows more or less the shape of the skull, we can apply this 3D deformation to the reference face and infer the face corresponding to the unknown skull.

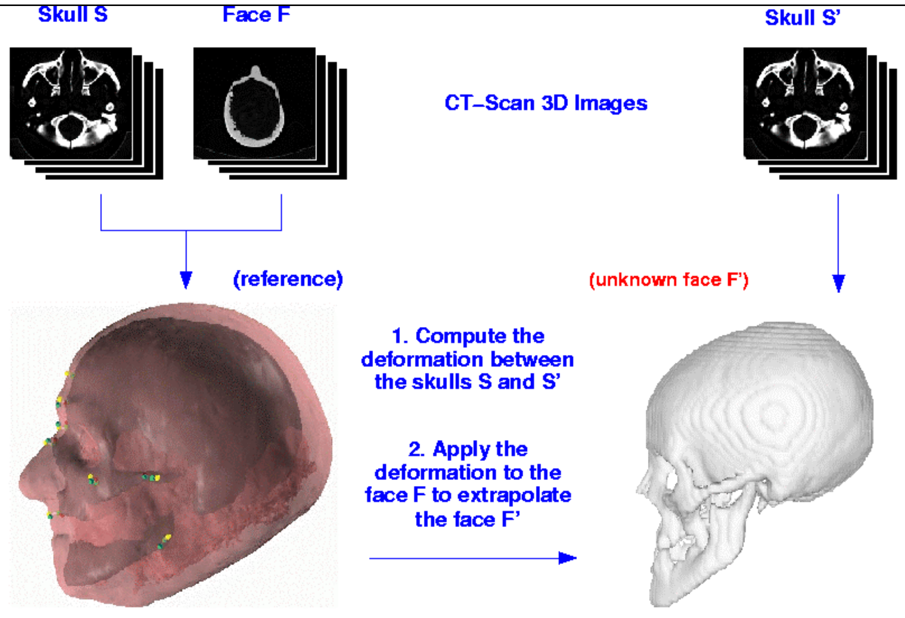

__Figure 10__: an automatic scheme for face reconstruction.
The two skulls are registered by using crest lines and the 3D deformation is applied to the reference face to infer the unknown face.

As a reference face, we use the CT-Scan of the mold of the face of the Modern Man (62 slices with a thickness of 3mm composed of 512 by 512 pixels of 0.6 by 0.6mm, data by courtesy of Gérald Quatrehomme, University of Nice, France) that we have aligned manually with the corresponding image of the skull (see Figure 11, left). We can see the result of the automatic reconstruction process in Figure 11, middle. In spite of using a face of an old person, whereas the Man of Tautavel was quite young, the result appears consistent with other facial reconstructions of the Man of Tautavel (see Figure 11, right).

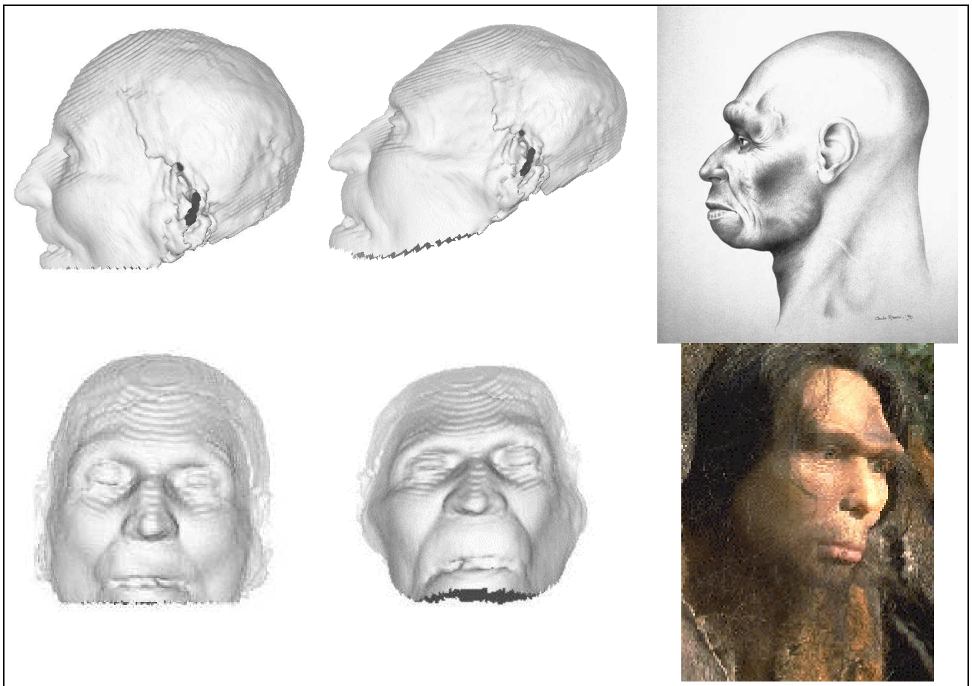

Figure 12*:automatic facial reconstruction of the Man of Tautavel.*
The automatic process deforms the reference face (left) to infer the face corresponding to the skull of the Man of Tautavel (middle).We can compare this reconstruction to the ones presented on the Web site (right):
http://www.culture.fr/culture/arcnat/tautavel/francais/hominter.htm

CONCLUSION

In this paper, we have presented several 3D image processing tools – feature extraction, feature registration, complex deformation computation – that can be combined in order to compute and analyze the deformation between two specimens. We have applied an entirely automatic methodology to the study of the shape of the skull of the Man of Tautavel and we present some preliminary results. Even if they have not yet been compared to the current established paleontology knowledge, we think that they are encouraging and assess the utility of such automatic tools, that are faster than manual procedures, that give reproducible results, and that can be easily parameterized to allow the paleontologist to test several hypotheses.

The development of such tools requires a close collaboration between physicians, anatomists, computer scientists morphometricians and paleontologists. We plan to improve all the steps of the scheme, especially the morphometric analysis. In particular, we will study how to decompose the 3D deformation into a small number of basic and “characteristic” deformations, as “relative warps” (Bookstein et al., 1999) or “principals warps” (Bookstein, 1991), (Ponce de León & Zollikofer, 2001).

We plan also to apply all this methodology to other anatomical structures as, for example, the human pelvis (Marchal, 2000) or animal bones (Rogers, 1999) and to study pathologic deformations (Mafart, 1998).

Endly, we will test our tools with 3D images acquired by new modalities as laser scanning (Kullmer et al., 2001) or Magnetic Resonance Imaging (Steiger, 2001).

AUTHORS

[1] Laboratoire d’Informatique, Université d’Avignon, France & Projet EPIDAURE, Institut National de Recherche en Informatique et en Automatique, Sophia Antipolis, France
[2] Laboratoire d’Anthropologie, Faculté de Médecine, UMR 6569, Université de la Méditerranée, Marseille, France
[3] Hôpital Militaire Robert Picqué, Bordeaux, France

Contact: Gérard Subsol – Laboratoire d'Informatique, Université d'Avignon
339, chemin des Meinajariès, Agroparc B.P. 1228 – 84911 Avignon Cedex 9, France
Gerard.Subsol@lia.univ-avignon.fr

REFERENCES

Ayache, N., 1998, L'analyse automatique des images médicales, état de l'art et perspectives. *Annales de l'Institut Pasteur*, vol. 9, no. 1, p. 13-21. Electronic version: http://www.inria.fr/rrrt/rr-3364.html

Bookstein, F.L., 1991, *Morphometric tools for landmark data*, Cambridge University Press.

Bookstein, F.L. & Cutting, C., 1988, A proposal for the apprehension of curving cranofacial form in three dimensions. In K. Vig et A. Burdi, eds., *Cranofacial Morphogenesis and Dysmorphogenesis*, p. 127-140, University of Michigan Press.

Bookstein, F.L., Schäfer, K., Prossinger, H., Seidler, H., Fieder, M., Stinger, C., Weber, G.W., Arsuaga, J.L., Slice, D.E., Rohlf, F.J., Recheis, W., Mariam, A.J. & Marcus, L.F., 1999, Comparing Frontal Cranial Profiles in Archaic and Modern *Homo* by Morphometric Analysis. *The Anatomical Record (New Anat.)*, 257, p. 217-224

Braun, M., Bouchet, P., Hublin, J.J. & Mallet, J.L., 1999, Les reconstitutions virtuelles des hommes préhistoriques. *Dossier Pour la Science : Les origines de l' humanité*, p. 78-81.

Conroy, G.C, Vannier, M.W. & Tobias, P.V., 1990, Endocranial Features of Australopithecus africanus Revealed by 2- and 3-D Computer Tomography. *Science*, vol. 247, p. 838-841.

Conroy, G.C., Weber, G.W., Seidler, H., Tobias, P.V., Kane, A. & Brunsden, B., 1998, Endocranial Capacity in an Early Hominid Cranium from Sterkfontein, South Africa. *Science*, vol. 280, p. 1730-1731.

Dean, D., 1993, *The Middle Pleistocene Homo erectus/Homo sapiens Transition: New Evidence from Space Curve Statistics*. Ph.D. Thesis, The City University of New York.

Declerck, J., Subsol, G., Thirion, J.P. & Ayache, N., 1995, Automatic retrieval of anatomical structures in 3D medical images. In N. Ayache, ed., *Computer Vision, Virtual Reality and Robotics in Medicine*, Lecture Notes in Computer Science 905, p. 153-162, Nice (France), Springer. Electronic version: http://www.inria.fr/rrrt/rr-2485.html

Kalvin, A.D., Dean, D. & Hublin, J.J., 1995, Reconstruction of Human Fossils. *IEEE Computer Graphics and Applications*, vol. 15, no 1, p. 12-14.

Kullmer, O., Schrenk, F., Bromage, T., Huck, M., 2001, (HOTPAD) Hominid Tooth Pattern Data-collection based on optical 3D Topometry. In *Colloquium on 3D Imaging for Paleoantrhopology and Prehistoric Archeology, XIVth Congress of the International Union for Prehistoric and Protohistoric Sciences*. Liège (Belgium).

de Lumley, H., de Lumley, M.A. & David, R., 1982, Découverte et reconstruction de l'Homme de Tautavel. In *1er congrès de paléontologie humaine*, tome 1, Nice (France).

Mafart, B., 1998, Le crâne romain d'Arles : une syphilis frontale et naso-palatine post-Colombienne, apport des nouvelles méthodes de datation C14 pour la paléopathologie. In *Bulletin et Mémoires de la Société d'Anthropologie de Paris n.s.*, t 10, 3-4, p. 333-344, 1998.

Mafart, B., Méline, D., Silvestre, A. & Subsol, G., 1999, *3D Imagery and Paleontology: Shape differences between the skull of Modern Man and that of Tautavel Man*. B. Hidoine, A. Paouri, designers and directors, video 451-452, Department of Scientific Multimedia Communication, INRIA. This movie was showed at the exhibition *Homo Erectus à la conquête du monde*, Musée de l'Homme, Paris in 1999-2000.
Electronic version: http://www.inria.fr/multimedia/Videotheque/0-Fiches-Videos/451-fra.html

Marchal, F., 2000, A new morphometric analysis of the hominid pelvic bone. *Journal of Human Evolution*, 38, p. 347-365.

Ponce de León, M.S. & Zollikofer, C.P.E., 1999, New Evidence from Le Moustier 1: Computer Assisted Reconstruction and Morphometry of the Skull. *The Anatomical Record*, 254, p. 474-489.

Ponce de León, M.S. & Zollikofer, C.P.E., 2001, Neanderhal cranial ontogeny and its implications for late hominid diversity. *Nature*, vol. 412, p. 534-537.

Quatrehomme, G., Cotin, S., Subsol, G., Delingette, H., Garidel, Y., Grevin, G., Fidrich, M., Bailet, P. & Ollier, A., 1997, A Fully Three-Dimensional Method for Facial Reconstruction Based on Deformable Models. *Journal of Forensic Sciences*, 42(4) p. 649-652.

Rae, T.C. & Koppe, T., 2000, Isometric scaling of maxillary sinus volume in hominoids. *Journal of Human Evolution*, 38 p. 411-423.

Rogers, S.W., 1999, Allosaurus, Crocodiles, and Birds: Evolutionary Clues from Spiral Computed Tomography of an Endocast. *The Anatomical Record (New Anat.)*, 257, p. 162-173.

Seidler, H., Falk, D., Stringer, C., Wilfing, H., Müller, G.B., zur Nedden, D., Weber, G.W., Reicheis, W., Arsuaga, J.L., 1997, A comparative study of stereolithographically modelled skulls of Petralona and Broken Hill : implications for future studies of middle Pleistocene hominid evolution. *Journal of Human Evolution*, 33, p. 691-703.

Spoor, F. & Zonneveld, F., 1995, Morphometry of the primate bony labyrinth : a new method based on high resolution computed tomography. *Journal of Anatomy*, 186, p. 271-286.

Spoor, F., Jeffery, N. & Zonneveld, F., 2000, Using diagnostic radiology in human evolutionary studies. *Journal of Anatomy*, 197, p. 61-76. Electronic version: http://evolution.anat.ucl.ac.uk/people/spoor/spmain.htm

Steiger, T., 2001, Nuclear magnetic resonance imaging in paleontology. *Computers & Geosciences*, 27, p. 493-495.

Subsol, G., 1995, *Construction automatique d'atlas anatomiques morphométriques à partir d'images médicales tridimensionnelles*. Ph.D. Thesis, École Centrale Paris. Electronic version: http://www.inria.fr/RRRT/TU-0379.html

Subsol, G., Thirion, J.P. & Ayache, N., 1998, A General Scheme for Automatically Building 3D Morphometric Anatomical Atlases : application to a Skull Atlas. *Medical Image Analysis*, 2(1), p. 37-60.

Subsol, G., Mafart, B., Méline, D., Silvestre, A. & de Lumley, M.A., 2000, Traitement d'images scanographiques appliqué à l'étude tridimensionnelle de l'évolution de la forme du crâne humain. In P. Andrieux, D. Hadjouis, A. Dambricourt-Malassé, eds., *L'identité humaine en question*, p. 92-101. Collection Paléoanthropologie et paléopathologie osseuse, Artcom.

Thirion, J.P. & Gourdon, A., 1996, The 3D Marching Lines Algorithm. *Graphical Models and Image Processing*, 58(6), p. 503-509. Electronic version: http://www.inria.fr/RRRT/RR-1881.html

Thirion, J.P., Subsol, G. & Dean, D., 1996, Cross Validation of Three Inter-Patients Matching Methods. In K.H. Höhne, R. Kikinis, eds., *Visualization in Biomedical Computing*, vol. 1131, Lecture Notes in Computer Science, p. 327-336, Hamburg (Germany), Springer.

Thirion, J.P., Prima, S., Subsol, G. & Roberts, N., 2000, Statistical Analysis of Normal and Abnormal Dissymmetry in Volumetric Medical Images. *Medical Image Analysis*, 4 p. 111-121.

Thompson, d'A.W., 1917, *On Growth and Form*. Bonner, J.T. ed,. Cambridge University Press (first edition in 1917).

Thompson, J.L. & Illerhaus, B., 1998, A new reconstruction of the Le Moustier 1 skull and investigation of internal structures using 3-D-µCT data. *Journal of Human Evolution*, 35, p. 645-667.

Weber, G.W., 2001, Virtual Anthropology (VA): A Call for Glasnost in Paleoanthropology. *The Anatomical Record (New Anat.)*, 265:193-201.

Zollikofer, C.P.E., Ponce de León, M.S. & Martin, R.D., 1998, Computer-Assisted Paleoanthropology. *Evolutionary Anthropology*, 6, p. 41-54.